International Journal of Engineering Research & Technology (IJERT)
ISSN: 2278-0181
Vol. 6 Issue 08, August - 2017

Punching of High Strength Concrete Flat Slabs without Shear Reinforcement

Mr Kiran Tukaram Shembade
Master of Engineering
N.B. Navale Sinhgad College of Engineering,
Kegaon, Solapur-413255 (M.S.) India.
Solapur University, Solapur

Abstract **- The experimental research carried out to study the punching behavior of high strength concrete (HSC) flat slabs is reported in the present work. Three flat slab specimens were cast using HSC and another one with normal strength concrete (NSC), to be used as a reference slab. The HSC mix presented a compressive strength of about 130 MPa, with a basalt coarse aggregate. The tested specimens were square with 1650 mm side and 125 mm thickness. The longitudinal reinforcement ratio varied between 0.94% and 1.48%. The experimental results show that the use of HSC led to a significant load capacity increase when compared with the reference model made with NSC. Furthermore, the experimental results also indicated that as the longitudinal reinforcement ratio increased, the punching capacity also increased. The results obtained in this set of experimental tests and others collected from the literature were compared with the code provisions by EC2, MC2010 and ACI 318-11.**

1. INTRODUCTION

Reinforced concrete flat slabs are a structural solution widelyused nowadays for office, commercial and residential buildings. They present several advantages such as the much reduced and simpler formwork, easy installation of mechanical and electrical infrastructures, the versatility and easier space partitioning and faster site operations, which makes flat slabs an economical and efficient structural system. However, they present a complex behavior which may lead to a punching failure. One of the most important subjects in the design of concrete flat slabs is the punching capacity, being frequently the governing factor in choosing its thickness.

The high strength concrete (HSC) technology has continuouslyevolved in the last few decades. In recent years the use of HSC has increased significantly for different structural applications such as bridges, offshore structures and buildings. Despite the growing use of HSC, the information available on its structuralperformance is reduced, particularly with concrete compressive strengths above 90 MPa, and the punching phenomenon is not an exception.

There are several experimental studies on the punching behavior of HSC slabs, but most of them adopted concrete with compressive strengths under 90 MPa[1–12]. In the referred, works only

nine specimens were tested wherein the concrete compressive strength was greater than 90 MPa and only five of them had more than 100 MPa. Previous works conducted to investigate punching shear behavior showed that increasing the concrete compressive strength resulted in an improvement in structural performance.The punching capacity increases with the increase in concrete strength and alongside the slab stiffness is also higher [13]. High strength concrete slabs usually exhibited a more brittle failure than normal strength concrete flat slabs.

2. EXPERIMENTAL RESEARCH

The experimental program consisted in testing four reinforcedconcrete flat slabs specimens, three with HSC and another one with normal strength concrete (NSC), under concentric and monotonic increasing punching load. The concrete strength used ranged between 35.9 MPa (NSC) and 130.1 MPa (HSC), while the average longitudinal reinforcement ratios varied between 0.94% and 1.48%.

The reduced scale specimens measured 1650 x1650 mm2, were 125 mm thick and intended to simulate the area near acolumn of an interior slab panel up to the zero moment's line (see Fig. 1).

The specimens were named based on concrete compressivestrength grade (SNSC for the normal strength concrete slabs and SHSC for high strength concrete specimens) and on its longitudinal reinforcement ratio. The reinforcement ratios of specimens SHSC1, SHSC2 and SHSC3, built with HSC, were 0.94%, 1.24% and 1.48%, respectively. Specimen used as reference, SNSC, was cast with NSC and

International Journal of Engineering Research & Technology (IJERT)
ISSN: 2278-0181
Vol. 6 Issue 08, August - 2017

Nomenclature

ρ	longitudinal reinforcement ratio	k_ψ	factor that depends on the deformations of the slab
ψ	slab rotation	m_R	average flexural strength per unit length in the support strip
ε_y	yield strain of steel reinforcement	m_s	moment per unit length for calculation of the flexural reinforcement in the support strip
c	column side dimension	r_s	distance between the column axis and the position of zero radial bending moment
d	average effective depth	u	length of the control perimeter
d_g	maximum aggregate size	E_c	modulus of elasticity of concrete
d_v	shear-resisting effective depth	E_s	modulus of elasticity of flexural reinforcement
f_c	mean value of cylinder compressive concrete strength	V_{exp}	experimental punching load
$f_{ct,sp}$	mean value of concrete splitting tensile strength	V_{flex}	flexural capacity of slab
f_t	tensile strength of steel reinforcement	V_{min}	minimum value between V_{flex} and V_R
f_y	yield stress of steel reinforcement	V_R	predicted punching resistance
k	scale factor according to EC2		
k_{dg}	factor taking into account the influence of the maximum aggregate size		

With a reinforcement ratio of 1.25%. During the manufacture of the specimens their mean effective depths (d) were measured and are presented in Table 1, where it is also presented the details of the top and bottom longitudinal reinforcements, along with its average longitudinal reinforcement ratio (q).

The top and bottom reinforcement layouts were orthogonal andparallel to the slab edge. The longitudinal reinforcement concrete clear cover of both faces was 20 mm.

The specimens were monotonically loaded at 0.25 kN/s rate upto failure using a hydraulic jack of 1000 kN capacity, centrally positioned under the slab. The column was simulated by means of a square steel plate with 200 mm sides and 50 mm thick. Eight points on the top of the slab were fixed to the strong floor of the laboratory using high steel strands and spreader beams according to Fig. 1.

4. MATERIALS

For the NSC, locally available crushed coarse limestone aggregate was used along with medium and fine sand. For the HSC mix, crushed coarse basalt aggregates were used, togetherwith medium and fine sand.

The HSC was produced using Portland cement type CEM I 52.5 R, while in the NSC mix was used Portland cement CEM II/B-L 32.5 N. Silica fume corresponding to 10% of the cement weight was added in the mixing process of the HSC to enhance its mechanical properties. Due to a particle size of only one hundredth of the size of the cement particles, the silica fume contributes to a denser material structure. This will effectively fill the free space between aggregates and cement particles. Furthermore, silica fume is also a pozzolanic material that reacts with the calcium hydroxide and forms cement gel which also contributes to a denser materialand to increase the hardened concrete strength [14]. Because of the low water cement ratio and to improve the workability, a superplasticizer was added during the mixing of the HSC. The materials quantities used in the concrete mixtures are presented in Table 2. The maximum aggregate size is of 13.9 mm and 13.2 mm, for the HSC and the NSC, respectively.

International Journal of Engineering Research & Technology (IJERT)
ISSN: 2278-0181
Vol. 6 Issue 08, August - 2017

The concrete compressive (fc) and splitting tensile (fct,sp) strength were determined on 150 x 300

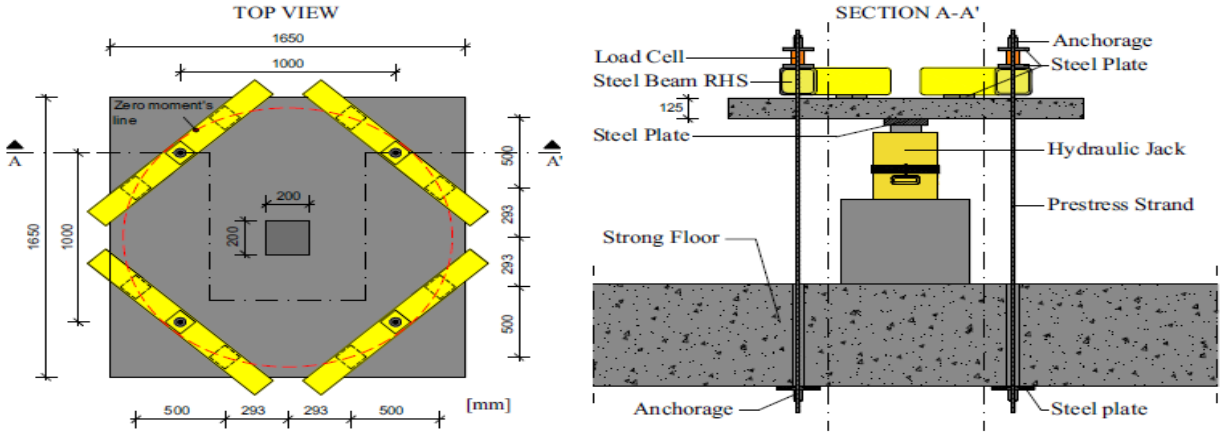

Fig. 1. Test setup.

mm cylinders, accordingto EN 12390-3 [15] and EN 12390-6 [16], respectively.

Specimen	d (mm)	Longitudinal reinforcement		q (%)
		Bottom	Top	
SHSC1	104.2	#8 bars φ 8//200 mm	#21 bars φ 10//80 mm	0.94
SHSC2	101.6	#8 bars φ8//200 mm	#17 bars φ 12//90 mm	1.24
SHSC3	101.7	#8 bars φ8//200 mm	#21 bars φ 12//75 mm	1.48
SNSC	100.7	#8 bars φ8//200 mm	#17 bars φ 12//90 mm	1.25

Table 1Main characteristics of specimen's reinforcement.

-=8888Cement	500 (CEM I 52.5 R)	320 (CEM II/B-L 32.5 N)
Silica fume	50	-
Coarse aggregate (8/16)	1088	906
Medium sand (2/4)	489	626
Fine sand (0/2)	245	286
Superplasticizer	8.43	-
Water	139.1	184.3

Table 2Concrete mix proportions (kg/m3).

The modulus of elasticity of concrete (Ec) was determined on compressiontests on 150 _ 300 mm cylinders, according to the E-397 [17]. The cylinders were first loaded to a stress of 1/3 fc and then unloaded down to 0.5 MPa. The modulus of elasticity was determined from the slop of the stress–strain curve registered in cycles between a stress of 0.5 MPa and 1/3 fc. The average values of compressive strength (fc), splitting tensile strength (fct,sp) and modulus of elasticity of concrete (Ec) are presented in Table 3.

In order to determine the yield stress (fy) and the tensilestrength (ft) of the longitudinal reinforcement, direct tensile tests were performed on coupons from the same steel batch, according to EN 10002-1 [18]. Those results are listed in Table 3.

5. INSTRUMENTATION

Loads and displacements were measured during the tests, as well as strains in the top longitudinal reinforcement bars, by means of an electronic data acquisition device connected to a computer.

The applied loads to the slabs were measured through the use offour load cells, one in each steel tendon fixing the slab to the strong floor of the laboratory. The vertical displacements of the slabs were measured at 11 points of the top surface using linear variable differential transformers (LVDT). LVDT D1 was placed in the center of the specimens. LVDTs D2 to D7 were placed in the direction of higher effective depth of the top longitudinal reinforcement, while LVDTs D8 to D11 were placed in the perpendicular direction, as show Fig. 2. Strains in several points of the top flexural reinforcement bars with higher effective depth were also measured, according to Fig. 3. In each measuring point two electrical resistance strain gauges diametrically opposed were glued to the bars. The measured strain value was computed as the mean value of the strains in these two strain gauges.

International Journal of Engineering Research & Technology (IJERT)
ISSN: 2278-0181
Vol. 6 Issue 08, August - 2017

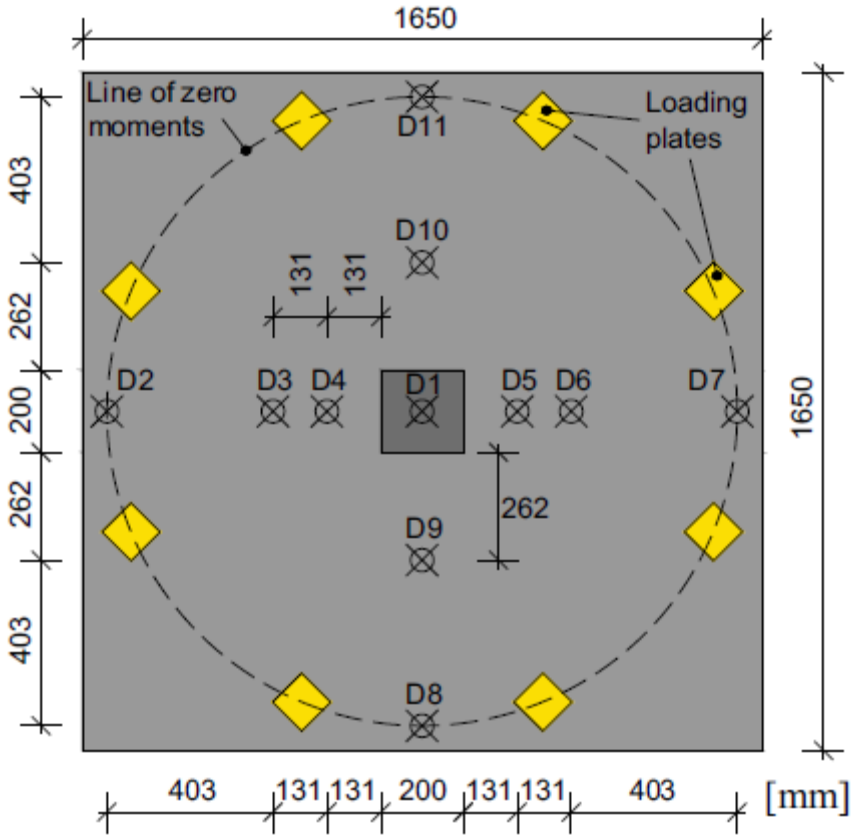

Fig. 2. LVDT's and loading plate's position

Specimen	Concrete (Mpa)			Top reinforcement (Mpa)		Bottom reinforcement(Mpa)	
	fc	fct,sp	Ec	fy	ft	fy	ft
SHSC1	125.6	7.7	54.4	511.8	643.9	549.7	697.3
SHSC2	130.1	8.4	55.5	523.4	671.4	549.7	697.3
SHSC3	129.6	8.3	54.4	523.4	671.4	549.7	697.3
SNSC	35.9	2.6	32.6	532.3	642.6	549.7	697.3

Table 3 Mechanical properties of concrete and reinforcement bars.

6. EXPERIMENTAL RESULTS

1. Vertical displacement

The load–deflection evolution, measured by means of 11 LVDTs placed on the top surface of the slabs, is presented in Fig. 4 for each specimen. These curves were obtained using the relative displacementscomputed between the measured value of LVDT placed on the center and the mean value of two opposite LVDTs. The initial load corresponds to the self-weight of specimens and test system equipment placed on the slab.

In the HSC specimens the beginning of the flexural cracking occurs for a load between 130 kN and 180 kN, while in the NSCbspecimen occurs for a load between 50 kN and 80 kN. This behavior is related to the higher tensile strength of HSC. As expected, the load–deflection curves were stiffer before flexural cracks start to form and develop. In the HSC specimens the increase of the longitudinal reinforcement ratio led to a vertical displacement decrease at failure, while the stiffness increased slightly.

2. Longitudinal reinforcement strains

Fig. 5 presents the evolution of top reinforcement strains for each specimen. The location of the strain gauges is presented in Fig. 3. The bar strains presented in Fig. 5 were obtained as the average value of the pair of strain gauges glued to each monitored bar. During the experimental test, the SG1-SG2 pair of specimen SHSC1 was damaged when the applied load reached about 350 kN, and for that reason the results for that pair of strain gauges are only

International Journal of Engineering Research & Technology (IJERT)
ISSN: 2278-0181
Vol. 6 Issue 08, August - 2017

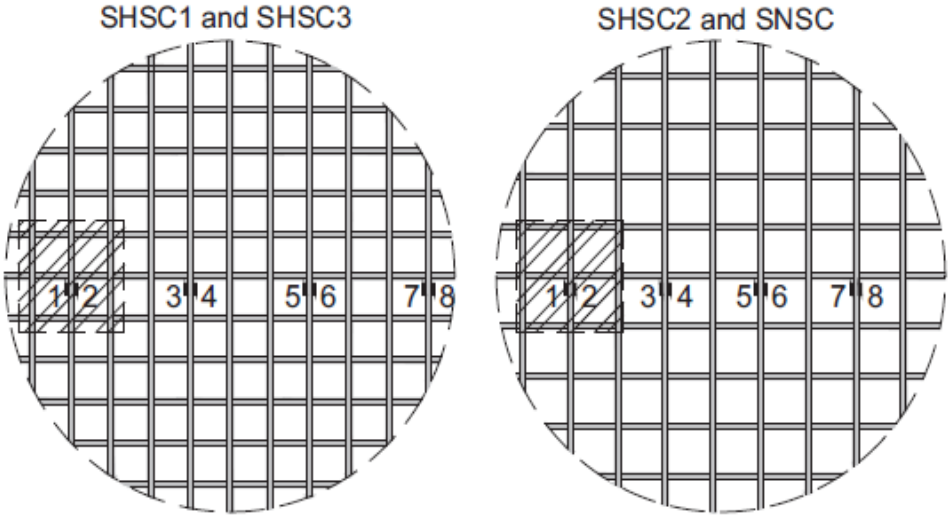

Fig. 3. Strain gauges position.

Presented until that load level. The yielding strains of the toplongitudinal reinforcement were computed using the strength properties of the top longitudinal reinforcement presented in Table 3 and considering a modulus of elasticity of 200 GPa, and were considered as about 2.46‰ for SHSC1 specimen, 2.62‰ for SHSC2 and SHSC3, and 2.66‰ for specimen SNSC. A dashed line marks the considered yield strain for each specimen in Fig. 5.

It can be observed that in some bars the strains show a sudden increase for a load level corresponding roughly to the beginning of the flexural cracking development. This is especially true for the HSC specimens. This behavior may be justified by the transfer of stresses between the tensioned concrete and the reinforcement bars that occur at moment of crack formation, which is higher for the HSC specimens.

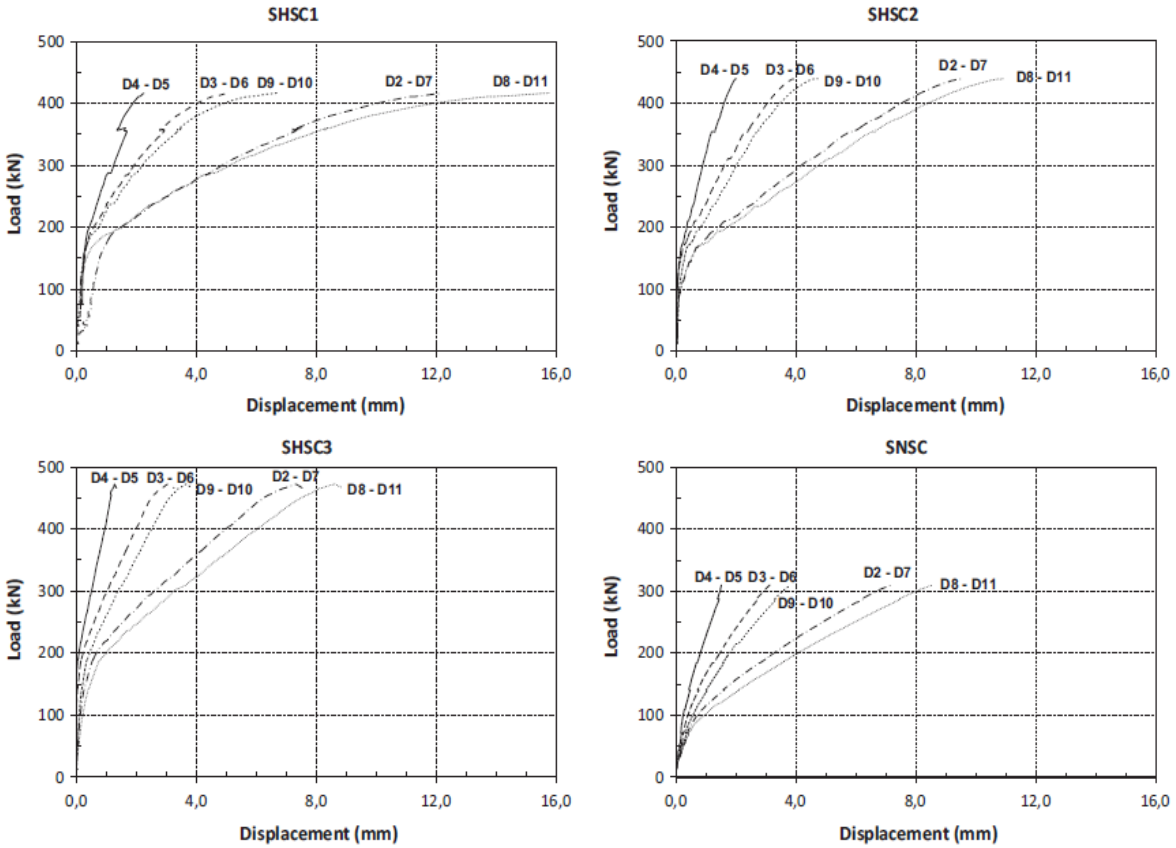

Fig. 4. Load–displacement graphs for all specimens.

International Journal of Engineering Research & Technology (IJERT)
ISSN: 2278-0181
Vol. 6 Issue 08, August - 2017

Considering the above mentioned values for the yield strain, in specimens SHSC1 and SHSC2, three of four monitored bars yielded, while in specimens SHSC3 only two shown that behavior. Nevertheless, the development of a full flexural yield line was not achieved in none of specimens. Also, as the reinforcement ratioincreased, the obtained strains at failure were smaller, as expected. In the SNSC specimen none of the monitored bars reached the yield strain, as shown into Fig. 5.

3. Slabs load capacity and failure mode

The experimental failure loads (Vexp) including self-weight of tested specimens are presented in Fig. 6. All specimens failed by punching. Failure patterns of the tested slabs are shown in Fig. 7.

Comparing specimens with similar longitudinal reinforcement ratio, SHSC2 and SNSC, made with HSC and NSC, respectively, an increment of load capacity of about 42% was obtained. In the specimens made with HSC, the ultimate punching load increases with the reinforcement ratio. The load capacity of specimen SHSC3, with a reinforcement ratio of 1.48%, was about 13% higher than the failure load of specimen SHSC1, which had a reinforcement ratio of 0.94%.

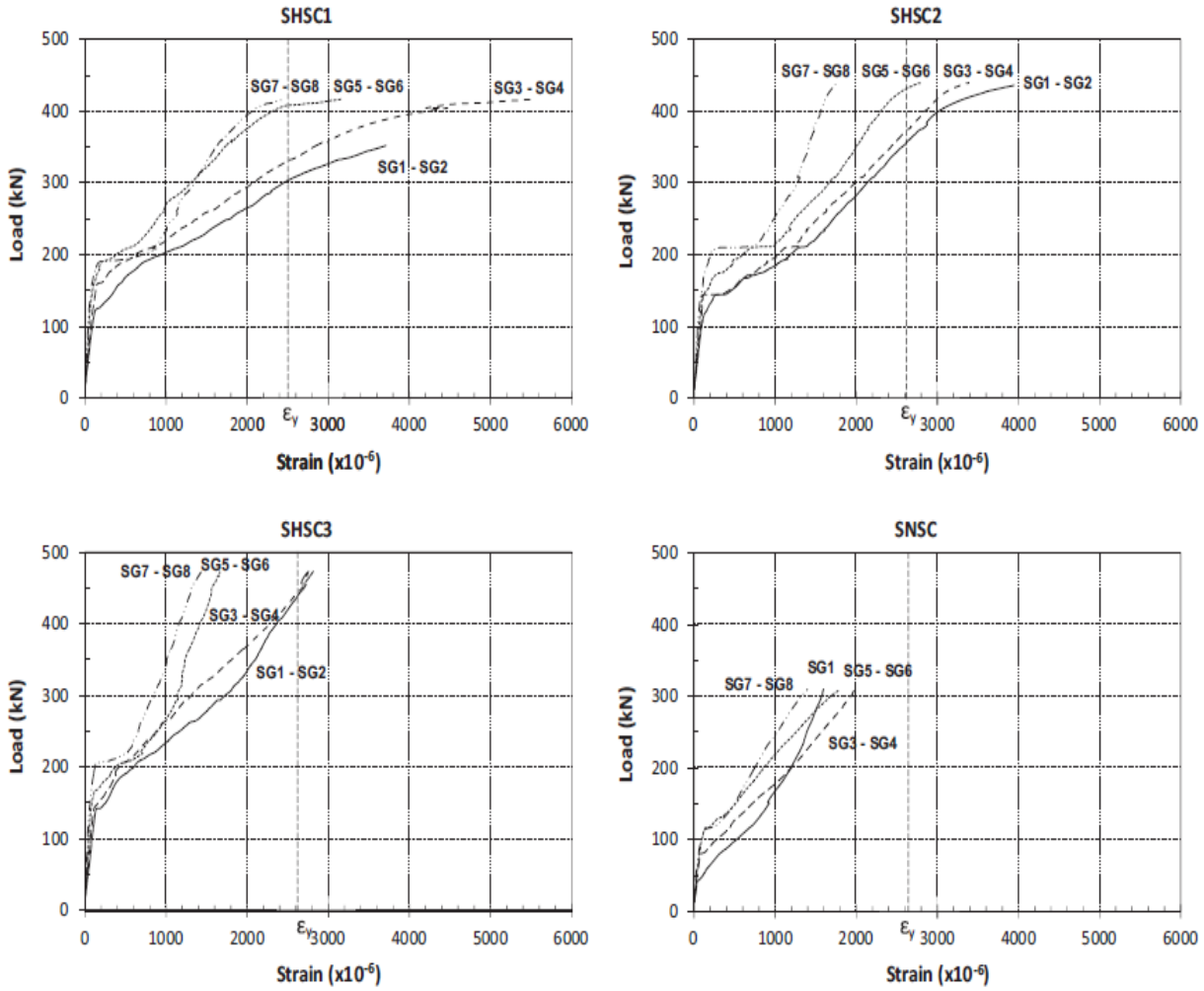

Fig. 5.Load–strain evolution on top reinforcement.

International Journal of Engineering Research & Technology (IJERT)
ISSN: 2278-0181
Vol. 6 Issue 08, August - 2017

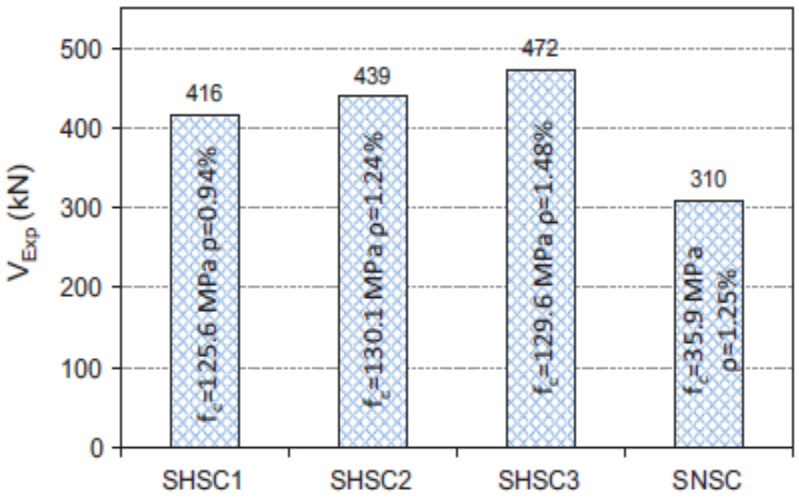

Fig. 6. Experimental failure loads.

The crack pattern at failure was similar for all specimens. However, for specimens cast with high strength concrete (SHSC1, SHSC2 and SHSC3) the number of observed cracks was higher. Furthermore, a considerablespalling of concrete cover was observed at failure for the HSC specimens, which indicates a more brittle behavior. In the specimens SHSC1 and SHSC2 evident flexural cracks were observed, in the direction perpendicular to the longitudinal top reinforcement with lower effective depth, which developed almost up to the edges of the slabs, but not achieving a full flexural yield line.

The tested specimens were cut after failure. Fig. 8 presents, for all specimens, pictures of the saw cut sections. After the cutting of the specimens it was possible to measure the failure surfaces inclination in both orthogonal directions and the average values are presented in Table 4.

7. COMPARISONS BETWEEN THE TESTS RESULTS AND CODE PREDICTIONS

In this section, the experimental failure loads obtained in this set of experimental tests and others collected from the literature are compared with the predictions of EC2 [19], MC2010 [20] and ACI 318-11 [21]. The predicted punching resistance was computed considering the mean values for the material properties and without considering the partial safety coefficients.

The punching resistance of slabs was computed by EC2 [19](VR,EC) through the following expression (Eq. (1)):

$$V_{R,EC} = 0.18 \cdot k \cdot (100 \cdot \rho \cdot f_c)^{1/3} \cdot u \cdot d \qquad (1)$$

where the reinforcement ratio values (q) are calculated taking into account a slab width equal to the column's width plus 3d each side and must not be higher than 2%; d is the mean effective depth of the top flexural reinforcement [in mm] and fc is the concrete cylinder strength in MPa. The control perimeter u is defined at a distance 2d from the column sides and constructed as to minimize its length and for the tested slabs is calculated as u = 4c + 4pd [in mm], where c is the cross-section dimension of a square column. The parameter k is a factor accounting for size effect whose value can be obtained by Eq. (2):

$$k = \left(1 + \sqrt{200/d}\right) \leqslant 2 \quad [d \text{ in mm}] \qquad (2)$$

According to MC2010 [20], for slabs without transverse reinforcement, the predicted punching loads can be computed by Eq. (3).

$$V_{R,MC} = k_\psi \cdot \sqrt{f_c} \cdot u \cdot d_v \qquad (3)$$

In MC2010 [20], the control perimeter u is defined at a distance of 0.5dv from the edge of the column, and constructed to minimize its length which for the tested slabs is given as u = 4c + pdv [in mm] where c is the cross-section dimension of a square column,dv is the shear-resisting effective depth [in mm] and fc is the concrete cylinder strength in MPa.

International Journal of Engineering Research & Technology (IJERT)
ISSN: 2278-0181
Vol. 6 Issue 08, August - 2017

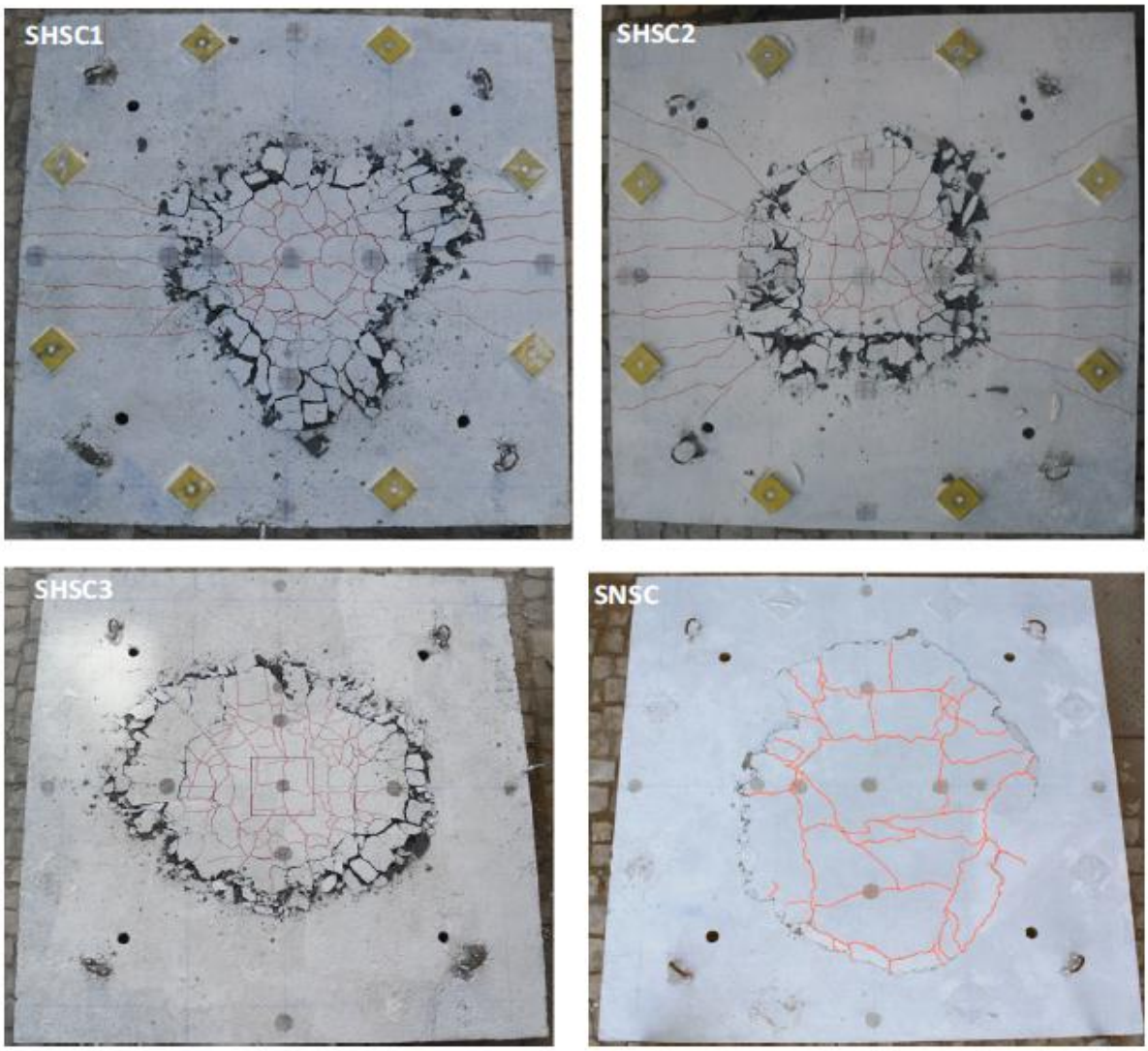

Fig. 7.Top view of specimens after failure.

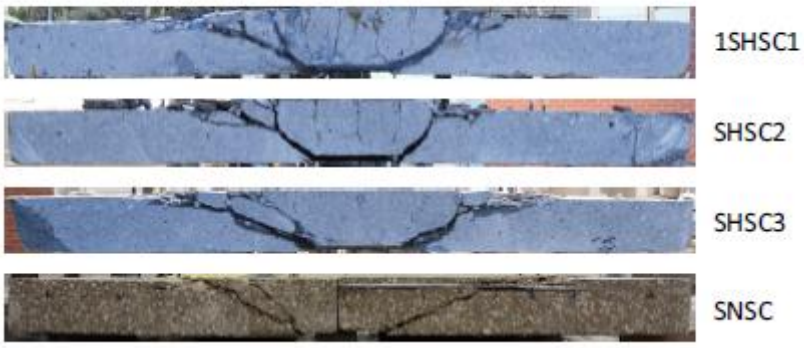

Fig. 8. Saw cuts of tested specimens

For the tested slabs, the shearresistingeffective depth dv is equal to d [in mm], being d the meaneffective depth of the top flexural reinforcement. The parameter kwdepends on the rotations of the slab around the support region andfollows from (Eq. (4)):

$$k_\psi = \frac{1}{1.5 + 0.9k_{dg} \cdot \psi \cdot d} \leqslant 0.6 \ [d \text{ in mm}] \qquad (4)$$

International Journal of Engineering Research & Technology (IJERT)
ISSN: 2278-0181
Vol. 6 Issue 08, August - 2017

wherein the parameter kdg is a factor taking into account the influence of the maximum aggregate size (dg) in the punching shear resistance and is assessed using (Eq. (5)):

$$k_{dg} = \frac{32}{16 + d_g} \geqslant 0.75 \ [d_g \text{ in mm}] \qquad (5)$$

For high strength concrete, MC2010 [20] recommends that dg should be assumed to be zero, because the aggregate particles may break, resulting in a reduced aggregate interlock contribution. The slab rotation (w) may be obtained for level III of approach by Eq. (6):

$$\psi = 1.2 \cdot \frac{r_s}{d} \frac{f_y}{E_s} \cdot \left(\frac{m_s}{m_R}\right)^{1,5} \text{ if } m_s \leqslant m_R \qquad (6)$$

where ms is calculated from a linear elastic model as the average value of the bending moment used for flexural reinforcement design over the width of the support [22]; mRis the average flexural strength per unit width in the support strip and rsstands for the position where the radial bending moment is zero with respect to the column axis.

SHSC1	SHSC2	SHSC3	SNSC
29	41	29	25

Table 4 Average inclination of failure surfaces.

EC2	MC2010		ACI 318-11
	dg = 0	Real dg	
Average	1.15	1.39	1.35
COV	0.14	0.09	0.19
5%	0.94	1.2	0.94

Table 6 Resumed results of the obtained relations Vexp/Vmin.

The punching resistance of flat slabs without transverse reinforcement and for square columns with side lengths less than 4d is given by ACI 318-11 [21] using (Eq. (7)):

$$V_{R,ACI} = \frac{\sqrt{f_c} \cdot u \cdot d}{3} \qquad (7)$$

International Journal of Engineering Research & Technology (IJERT)
ISSN: 2278-0181
Vol. 6 Issue 08, August - 2017

Table 5
Comparison between experimental punching results and code provisions.

Specimen	f_c (MPa)	d (mm)	ρ (%)	V_{exp} [a] (kN)	V_{flex} [b] (kN)	V_{exp}/V_{min} [c]			
						EC2	MC2010 ($d_g = 0$)	MC2010 (real d_g)	ACI 318-11
SHSC1	125.6	104.2	0.94	415.9	411.0	1.07	1.32	1.09	1.01[A]
SHSC2	130.1	101.6	1.24	439.2	530.9	1.06	1.26	1.04	0.94
SHSC3	129.6	101.7	1.48	472.4	637.9	1.08	1.25	1.04	1.01
SNSC	35.9	100.7	1.25	309.6	507.8	1.16	–	1.13	1.28
Marzouk and Hussein [2]									
HS1	67	95	0.49	178	185.5	0.96[A]	1.15	0.96[A]	0.96[A]
HS2	70	95	0.84	249	314.3	1.04	1.23	0.97	0.96
HS3	69	95	1.47	356	537.0	1.24	1.40	1.14	1.38
HS4	66	90	2.37	418	746.2	1.38	1.54	1.30	1.79
HS5	68	125	0.64	365	416.4	1.06	1.31	1.03	0.97
HS6	70	120	0.94	489	560.2	1.33	1.57	1.26	1.35
HS7	74	95	1.19	356	440.8	1.30	1.49	1.20	1.33
HS8	69	120	1.11	436	655.0	1.13	1.31	1.06	1.22
HS9	74	120	1.61	543	936.0	1.21	1.38	1.14	1.46
HS10	80	120	2.33	645	1329.5	1.24	1.41	1.20	1.67
HS11	70	70	0.95	196	192.2	1.30	1.50	1.18	1.14
HS12	75	70	1.52	258	302.4	1.43	1.58	1.27	1.45
HS13	68	70	2.00	267	387.6	1.39	1.52	1.25	1.58
HS14	72	95	1.47	498	572.3	1.48	1.60	1.29	1.47
HS15	71	95	1.47	560	615.6	1.45	1.53	1.22	1.33
Tornaszewicz [3]									
nd65-1-1	64.3	275	1.49	2050	5248.2	1.15	1.43	1.22	1.47
nd95-1-1	83.7	275	1.49	2250	5330.8	1.15	1.44	1.21	1.41
nd95-1-3	89.9	275	2.55	2400	8858.6	1.00	1.25	1.09	1.45
nd115-1-1	112	275	1.49	2450	5400.0	1.14	1.43	1.20	1.33
nd65-2-1	70.2	200	1.75	1200	3137.3	1.08	1.40	1.20	1.53
nd95-2-1	88.2	200	1.75	1100	3184.3	0.92	1.18	1.01	1.25
nd95-2-3	89.5	200	2.62	1450	4645.0	1.05	1.36	1.20	1.64
nd95-2-1D	86.7	200	1.75	1300	3181.1	1.09	1.41	1.20	1.50
nd95-2-3D	80.3	200	2.62	1250	4598.5	0.94	1.22	1.08	1.49
nd95-2-3D+	98	200	2.62	1450	4680.3	1.02	1.32	1.15	1.57
nd115-2-1	119	200	1.75	1400	3231.7	1.05	1.37	1.16	1.38
nd115-2-3	108.1	200	2.62	1550	4714.9	1.05	1.36	1.19	1.60
nd95-3-1	85.1	88	1.84	330	781.5	1.28	1.34	1.17	1.62
Hallgren [4]									
HSC0	90.3	200	0.80	965.0	1402.1	0.98	1.48	1.17	1.08
HSC1	91.3	200	0.80	1021.0	1368.6	1.03	1.57	1.24	1.13
HSC2	85.7	194	0.82	889.0	1302.2	0.96	1.45	1.15	1.06
HSC4	91.6	200	1.19	1041.0	1912.8	0.92	1.34	1.08	1.15
HSC6	108.8	201	0.60	960.0	1057.4	1.00	1.61	1.25	0.97
HSC9	84.1	202	0.33	565.0	591.3	0.96	1.36	1.05	0.96[A]
Ramdane [5]									
1	88.24	98	0.60	224.0	271.8	0.99	1.20	1.03	0.94
6	101.6	98	0.60	233.0	272.5	0.99	1.20	1.03	0.91
12	60.4	98	1.30	319.0	564.7	1.24	1.38	1.23	1.61
14	60.8	98	1.30	341.0	564.9	1.32	1.47	1.31	1.72
16	98.4	98	1.30	362.0	578.4	1.20	1.34	1.18	1.43
22	84.24	98	1.30	405.0	673.8	1.41	1.54	1.27	1.73

[a] Experimental failure load.
[b] Predicted flexural failure load.
[c] $V_{min} = \min(V_{flex}; V_R)$.
[A] Value obtained using V_{flex}.

International Journal of Engineering Research & Technology (IJERT)
ISSN: 2278-0181
Vol. 6 Issue 08, August - 2017

Where the control perimeter u is defined at a distance of 0.5d fromthe edge of the column and is given as u = 4 (c + d) [in mm], fc is the concrete cylinder strength in MPa and d is the mean effective depth of the top flexural reinforcement [in mm].

8. COMPARISONS OF EXPERIMENTAL AND PREDICTED PUNCHING LOADS

To make a broader study, along with the experimental test data presented within this work, a total of additional 40 test results of slabs without shear reinforcement, tested on studies conducted by Marzouk and Hussein [2], Tomaszewicz[3], Hallgren[4] and Ramdane[5] were compared to the predicted values of punchingstrength computed using EC2 [19], MC2010 [20] and ACI 318-11 [21]. A brief description of the research studies is given below.

Marzouk and Hussein [2] tested 15 square slabs made with HSC with compressive strength between 66 and 80 MPa. The tested specimens were square with 1700 mm width and with a 150 mm square column in the center. They had different thicknesses (90, 120 and 150 mm) and reinforcement ratios varying between 0.49% and 2.33%.

Tomaszewicz[3] tested 13 square flat slab specimens supported along the edges and loaded at mid-span by a concentrated load up to failure by punching. The concrete strength of HSC varied between 64 MPa and 112 MPa. The variables in the specimens were the slab dimensions (3000, 2600 and 1500 mm), slab thicknesses(320, 240 and 120 mm), column dimensions (200, 150 and 1400 mm) and reinforcement ratio (1.49–2.62%).

Hallgren[4] conducted an experimental investigation to study the punching shear capacity and the structural behavior of HSC slabs with and without shear reinforcement. The tested specimens were circular with 2540 mm diameter and 240 mm thick, supported on circular concrete column stubs with 250 mm diameter. The concrete compressive strengths of slabs varied between 84 MPa and 109 MPa.

In 1996, Ramdane[5] tested 6 circular slabs, 125 mm thick and 1700 mm diameter, to study the punching behavior of HSC flat slabs without shear reinforcement. Slabs were made using concrete with a compressive strength between 61 and 102 MPa and had different reinforcement ratio (0.60% and 1.30%).

Table 5 presents the obtained results, including the experimental failure loads and the ratio between the experimental failure loads and the code predictions using the methods of EC2 [19], MC2010 [20] and ACI 318-11 [21]. Table 6 summarizes the obtained results, presenting the average, COV (coefficient of variation) and the 5% percentile of the Vexp/Vminratios, considering the specimens cast using HSC. The slabs where the predicted flexural capacity is smaller than the punching capacity were not considered in the values presented in Table 6. Also graphs with Vexp/VR in function of the concrete compressive strength, including trend lines, are presented in Fig. 9.

According to ACI 318-11 [21], due to limited test data on twowayshear strength of HSC slabs and lack of practical experienceon concretes with compressive strengths above 70 MPa, is imposed
a maximum value for concrete compressive strength (fc) of about 69 MPa to be used on Eq. (7). Also MC2010 [19] presents a compressive strength concrete limit of 120 MPa. Although the values of concrete compressive strength of slabs tested within this work and some of slabs from the literature review are greater than the referred limitations it was decided to use these codes to predict the punching capacity, but without considering those limitations. When using the MC2010 [20] and for the HSC specimens, in addition to compute the punching resistance considering the maximum aggregate size (dg) equal to zero, as recommended in MC2010 [20], it was decided to include also the values obtained using the real aggregate size.

From the results presented in Tables 5 and 6, it may be observed that EC2 [19] and MC2010 [20], considering in the last one the real maximum aggregate size, provides predicted punching resistance values close to those obtained experimentally, with an average ratio for Vexp/Vmin of 1.15 and 1.16, respectively. The mean values of the ratio Vexp/Vmin computed by ACI 318-11 [21] and MC2010 [20], considering in the last one the maximum aggregate size equal to zero for the HSC slabs are relatively high. Analyzing Fig. 9, all the codes considered shows a tendency to overestimate the punching capacity with the increase of the concrete compressive strength, being this more evident for the ACI 318-11. The scatter is highest for the ACI 318-11, being the smallest scatter obtained using MC2010 with the actual maximum aggregate size.

When considering the 5% percentile, the EC2 [19] and ACI 318-11 [21] give values below 1.0, meaning slightly unsafe estimates. The MC2010 [20], in the two scenarios considered, is always conservative.

The predicted values computed using MC2010 [19] show that using the maximum aggregate size instead of considering the maximum aggregate size equal to zero in Eq. (5), leads to a better estimate of HSC slabs load capacity, closer to the experimental failure loads and with a 5% percentile of 1.03.

Fig. 10 presents the comparison of experimental results and the characteristic failure criterion of MC2010 [20] given by Eqs. (3)–(6), where the punching shear strength is defined as function of the width of the critical shear crack. The tests results from the studies conducted by Ramdane[5] and Tomaszewicz[3] are not presented here because the rotation of slabs at failure was not available. Also the experimental rotation at failure of the slab HSC6 of Hallgren[4] and slabs HS1 and HS11 of Marzouk and Hussein [2] are also not available. The experimental values obtained considering the real dg are presented with filled dots and the results considering dg equal to zero are presented with empty dots. Observing Fig. 10, it is clear that considering the real value for themaximum aggregate size used in HSC leads to a better agreement with the failure criterion given by MC2010 [20].

International Journal of Engineering Research & Technology (IJERT)
ISSN: 2278-0181
Vol. 6 Issue 08, August - 2017

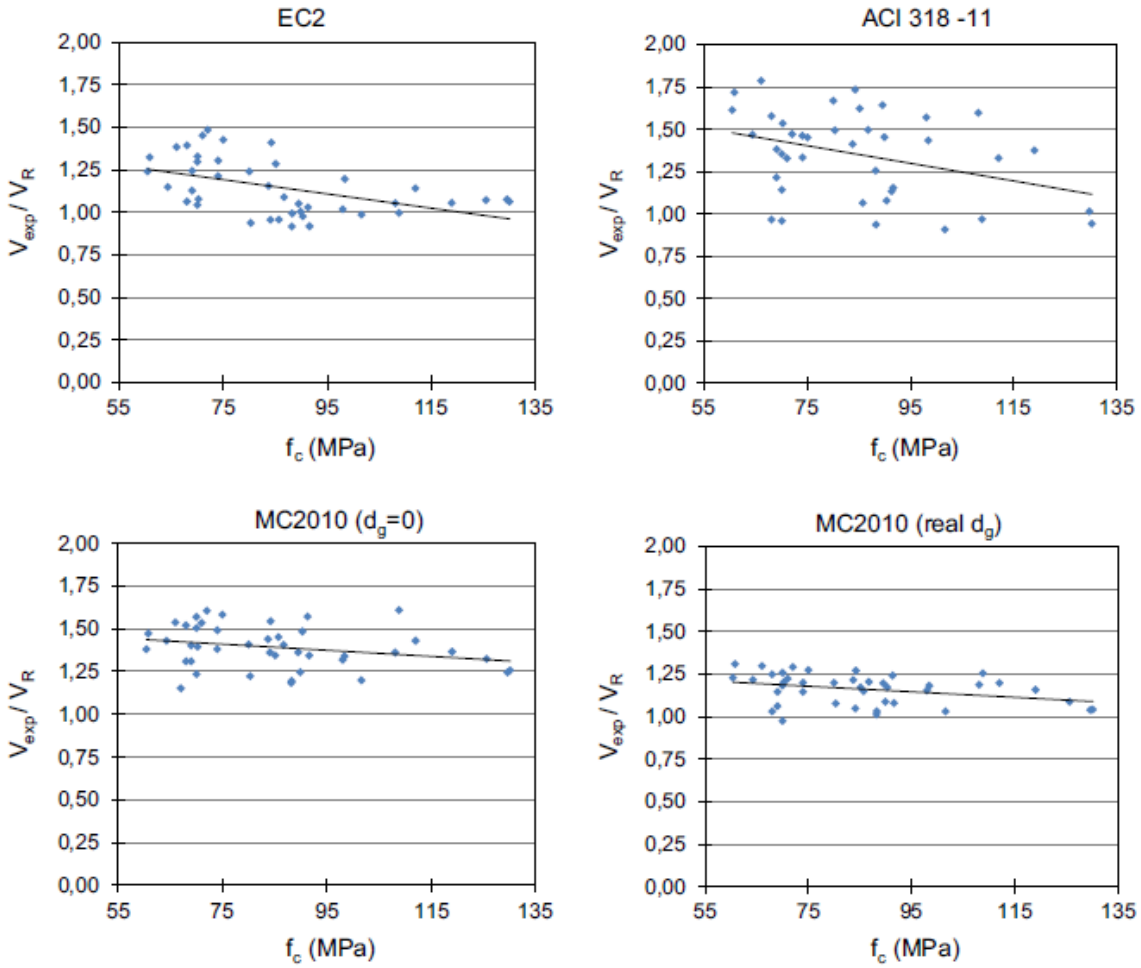

Fig. 9.Ratio Vexp/VR as a function of fc.

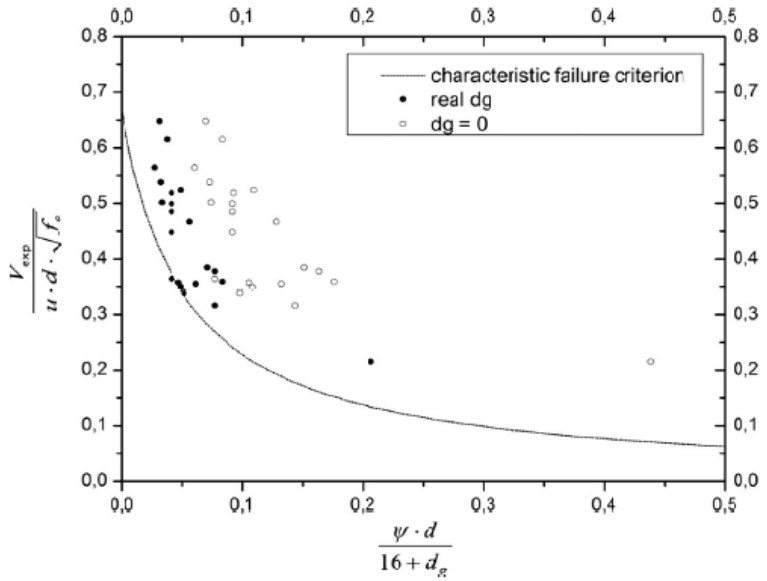

Fig. 10.Comparison between characteristic failure criterion of MC2010 and experimental results.

International Journal of Engineering Research & Technology (IJERT)
ISSN: 2278-0181
Vol. 6 Issue 08, August - 2017

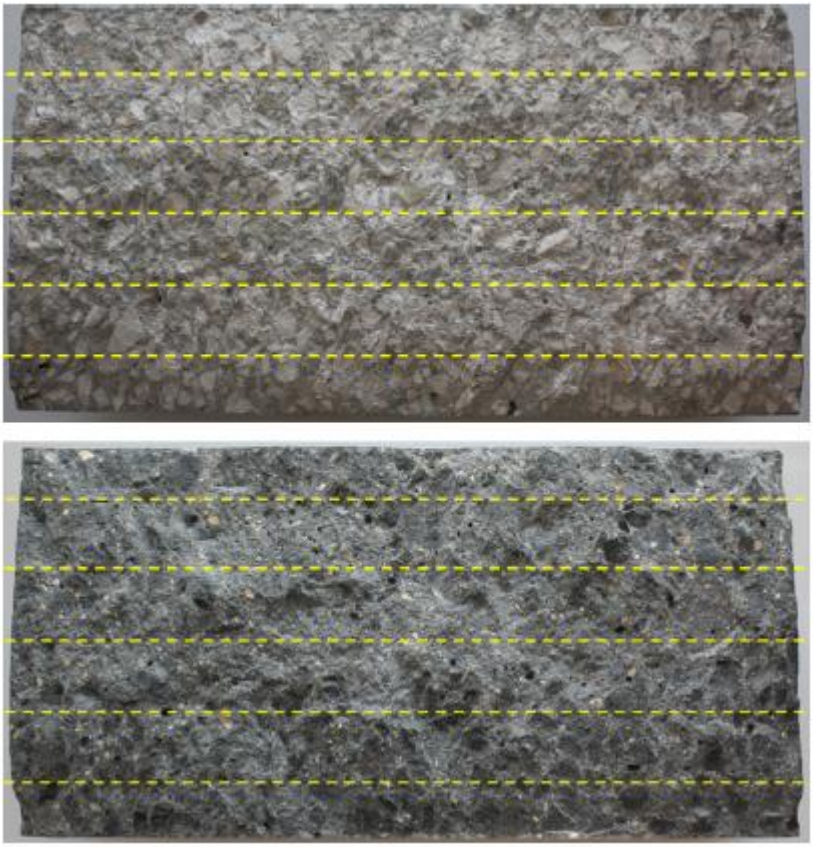

Fig. 11.Cylinder's failure surface of NSC (top) and HSC (bottom).

The amount of shear that can be transferred across the critical shear crack depends on the roughness of the crack, which in its turn is influenced by the maximum aggregate size [22]. The recommendation to use dg equal to zero for HSC is due to the believe that the failure surface of HSC may be smoother, which is not the case of the tested slabs. For the concretes used in this work the roughness of the failure surface was measured, in the half cylinders that resulted from the splitting tests. The roughness was measured by means of a laser displacement sensor with a resolution of 0.05 mm. For each half cylinder, the surveying of five longitudinal profiles spaced 25 mm was carried out. Fig. 11 presents the failure surface of HSC and NSC cylinders after the splitting test where the location of the considered longitudinal profiles is marked by a dash line.

The most common parameters to characterize the surface roughness are the total height of the roughness profile (Rt) and the average roughness (Ra) which represents the average deviation of the profile from a mean line (_y) and can be calculated using Eq. (8):

$$R_a = \frac{1}{n}\sum_{i=1}^{n}|y_i - \bar{y}| \qquad (8)$$

where n is the total number of samples points evaluated in the sampling length l and yi represents the absolute value of the profile deviation from the mean line, as shown in Fig. 12. The mean values

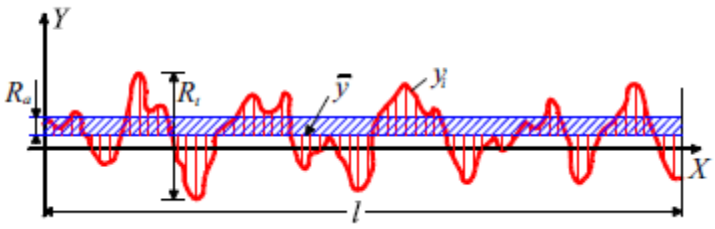

Fig. 12.Schematic surface profile; definition of parameters Ra and Rt.

International Journal of Engineering Research & Technology (IJERT)
ISSN: 2278-0181
Vol. 6 Issue 08, August - 2017

of Ra and Rt were 2.02 mmand 9.31 mmfor HSC, while for NSC were of 0.86 and 7.19, respectively. The presented values for the roughness parameters (Ra and Rt) show that the failure surface of the HSC used is even slightly rougher than for NSC. The values presented are valid for the type of course aggregate used, howevermay not occur for all HSC, especially for HSC made with aggregate of rock with lower strength than basalt.

CONCLUSIONS

This paper presents an experimental investigation undertaken to evaluate the punching behavior of HSC flat slabs. Three reduced scale flat slab specimens cast with HSC and another one cast with NSC were tested up to failure by punching. The experimental results are analyzed and compared with code provisions, along with the experimental results of 40 slabs made in HSC collected from literature. The main conclusions of this paper are:

1. Concrete strength has a direct influence on the punching behavior and the punching capacity. In fact, as the concrete compressive strength increases from about 36 MPa to 130 MPa, the punching capacity increased 42%, when comparing the tested slabs with longitudinal reinforcement ratios of 1.25%.
2. Test results showed that an increase of reinforcement ratio from 0.94% to 1.48% led to an increase in the punching capacity of about 13%.
3. The increase of the longitudinal reinforcement ratio led to smallerdisplacements at failure and to a stiffer behavior.
4. The concrete surface roughness that resulted from the splitting tests is slightly higher for the used HSC than for NSC.
5. Values computed using MC2010 [20], but considering the actual maximum aggregate size, leads to better punching resistance estimates and smaller scatter than the ones using the maximum aggregate size equal to zero, as recommended in MC2010 [20].
6. All the codes considered shows a tendency to overestimate the punching capacity with the increase of the concrete compressive strength, being this more evident for the ACI 318-11, although the compressive strength of most of the presented slabs are outside of its range of applicability. The data scatter is also the highest for ACI 318-11.
7. When considering the 5% percentile for the ratio between the experimental and the predicted failure capacity, the EC2 [19] and ACI 318-11 [21] give values below 1.0, meaning slightly unsafe estimates. The MC2010 [20], in the two scenarios considered, is always conservative.

REFERENCES

[1] Gardner NJ. Relationship of the punching shear capacity of reinforced concrete slabs with concrete strength. ACI Struct J 1990;87(5):66–71 [AmericanConcrete Institute, Detroit].
[2] Marzouk H, Hussein A. Experimental investigation on the behavior of highstrength concrete slabs. ACI Struct J 1991;88(6):701–13.
[3] Tomaszewicz A. Punching shear capacity of reinforced concrete slabs. Highstrength concrete SP2 – plates and shells. Report 2.3. Report no. STF70A93082. Trondheim: SINTEF; 1993. 36 pp.
[4] Hallgren M. Punching shear capacity of reinforced high strength concrete slabs. Doctoral thesis. Stockholm: Royal Institute of Technology; 1996. 206 pp.
[5] Ramdane KE. Punching shear of high performance concrete slabs. In: 4thinternational symposium on utilization of high-strength/high-performance concrete, Paris; 1996. p. 1015–26.
[6] Vargas ENZ. PunçãoemLajesCogumelo de Concreto de Alta ResistênciaReforçado com Fibras de Aço. Master thesis. Universidade de São Paulo; 1997. 244 pp.
[7] Marzouk H, Jiang D. Experimental investigation on shear enhancement types for high-strength concrete plates. ACI Struct J 1997;94(1):49–58.
[8] Ghannoum CM. Effect of high-strength concrete on the performance of slab column specimens. Doctoral thesis. Montréal: McGill University; 1998. 103 pp.
[9] Marzouk H, Emam M, Hilial MS. Effect of high-strength concrete slab on the behavior of slab-column connections. ACI Struct J 1998;95(3):227–36.
[10] Abdel Hafez AM. Punching shear behavior of normal and high-strength concrete slabs under static loading. J EngSci 2005;33(4):1215–35.
[11] Ozden S, Ersoy U, Ozturan T. Punching shear tests of normal and high strength concrete flat plates. Can J CivEng 2006;33(11):1389–400.
[12] Yasin ISB, Smadi MM. Behavior of high-strength fibrous concrete slab column connections under gravity and lateral loads. Constr Build Mater 2007;22:1863–73.
[13] Mamede N, Ramos A, Faria D. Experimental and parametric 3D nonlinear finite element analysis on punching of flat slabs with orthogonal reinforcement. EngStruct 2013;48:442–57.
[14] Magnusson J. Structural concrete elements subjected to air blast loading. Licentiate thesis, Stockholm; May 2007.
[15] European Committee for standardization. NP EN 12390-3. Testing hardened concrete – Part 3: compressive strength of test specimens; 2001.
[16] European Committee for standardization. NP EN 12390-6. Testing hardened concrete – Part 3: tensile splitting strength of test specimens; 2001.
[17] LNEC. E397 hardened concrete – determination of the modulus of elasticity of concrete in compression, Lisboa.
[18] European Committee for standardization. NP EN 10002-1. Metallic materials. Tensile testing – Part 1: method of test; 1990.